J. Phys. D: Appl. Phys. **32** (1999) 1768–1772. Printed in the UK PII: S0022-3727(99)02998-8

InAsSb/InAsSbP light emitting diodes for the detection of CO and CO_2 at room temperature

H H Gao†, A Krier†, V Sherstnev‡§ and Y Yakovlev‡

† Department of Physics, Lancaster University, Lancaster LA1 4YB, UK
‡ Ioffe Physico-Technical Institute, St. Petersburg, 195279, Russia

Received 25 March 1999

Abstract. This report describes the epitaxial growth and fabrication of room-temperature $InAs_{0.89}Sb_{0.11}/InAs_{0.48}Sb_{0.22}P_{0.30}$ semiconductor light emitting diodes operating in the mid-infrared wavelength region near 4.5 μm. The $InAs_{0.89}Sb_{0.11}$ ternary material used in the light emitting diode active region has a large lattice mismatch with respect to the InAs substrate layer and in order to accommodate this it was necessary to grow a buffer layer with an intermediate composition ($InAs_{0.94}Sb_{0.06}$). The devices exhibit infrared emission at 4.5 μm and could be effectively used as the basis of an optical sensor for the environmental monitoring of carbon monoxide at 4.6 μm and carbon dioxide at 4.2 μm in various applications.

1. Introduction

There is increasing interest in the fabrication of mid-infrared optoelectronic devices for a variety of practical applications including optical gas sensor instrumentation. In this respect there is a need for a compact and efficient semiconductor light source which can provide emission beyond the cut-off wavelength ($\sim$4 μm) of the glass envelope of a conventional filament bulb [1]. At the moment there are several different approaches which are being investigated for the fabrication of mid-infrared light emitting diodes (LEDs). These include molecular beam epitaxy (MBE) growth of type-II quantum wells [2] and strained-layer structures [3], metal–organic vapour phase epitaxy (MOVPE) growth of strained-layer superlattices and multi-quantum well (MQW) [4] and the more complex quantum cascade structures [5, 6] which have been successful at longer wavelengths but may be expensive to manufacture. In our laboratory we are interested in the liquid phase growth of narrow-gap semiconductor devices and have already produced LEDs which operate at some of the key wavelengths for gas detection [7–9]. Liquid phase epitaxy (LPE) has the advantage that it is an equilibrium growth technique and can cost-effectively produce room-temperature devices with good quantum efficiency and output power. Recent results in the literature [10–12] clearly demonstrate this capability. In the present work we report our first investigations of 4.5 μm LEDs based on $InAs_{1-x}Sb_x$/InAsSbP heterostructures corresponding to the composition $x \sim 0.1$ which is appropriate for the environmental monitoring of carbon dioxide (CO_2) and carbon monoxide (CO) using infrared optical techniques [13]. $InAs_{1-x}Sb_x$ of various compositions has been successfully grown using LPE [6, 14, 15], MBE [2, 16, 17] and MOVPE [18, 19]. We have previously reported high-quality lattice-matched $InAs_{0.91}Sb_{0.09}$ epilayers grown from Sb-rich melts onto lattice-matched GaSb substrates with efficient photoluminescence and good electrical transport properties [7, 15]. Although growth from Sb solution onto GaSb avoids the problem of substrate erosion during epilayer nucleation the associated thermodynamics restricts the epitaxy to a relatively narrow range of experimental growth conditions [14, 15]. The growth of suitable wide-gap heterojunction confinement layers is also problematic and therefore there is some advantage in re-considering growth from In-solution onto InAs substrates. This approach has the difficulty of significant lattice-mismatch, which is 0.76% between the InAs substrate and our proposed $InAs_{0.89}Sb_{0.11}$ active layer which is required for room-temperature emission at 4.5 μm. In this paper we investigate the effectiveness of using an $InAs_{0.94}Sb_{0.06}$ buffer layer of intermediate composition to alleviate this problem and its effect on the device characteristics of $InAs_{0.48}Sb_{0.22}P_{0.30}/InAs_{0.89}Sb_{0.11}/InAs_{0.48}Sb_{0.22}P_{0.30}$ double heterojunction LEDs.

2. Experimental procedures

A conventional horizontal, multi-well graphite sliding boat was used for the LPE growth of the LED structures. Epitaxy was carried out with the boat inside a high-purity quartz reactor tube under flowing purified hydrogen gas from a Pd-diffusion unit. The apparatus was fully automated and controlled with *Labview* operating software from a PC. This enabled convenient and reproducible multilayer epitaxy. The LED structures were grown onto 1 cm $\times$ 1 cm n-type

§ Royal Society visiting research fellow.

0022-3727/99/151768+05$30.00

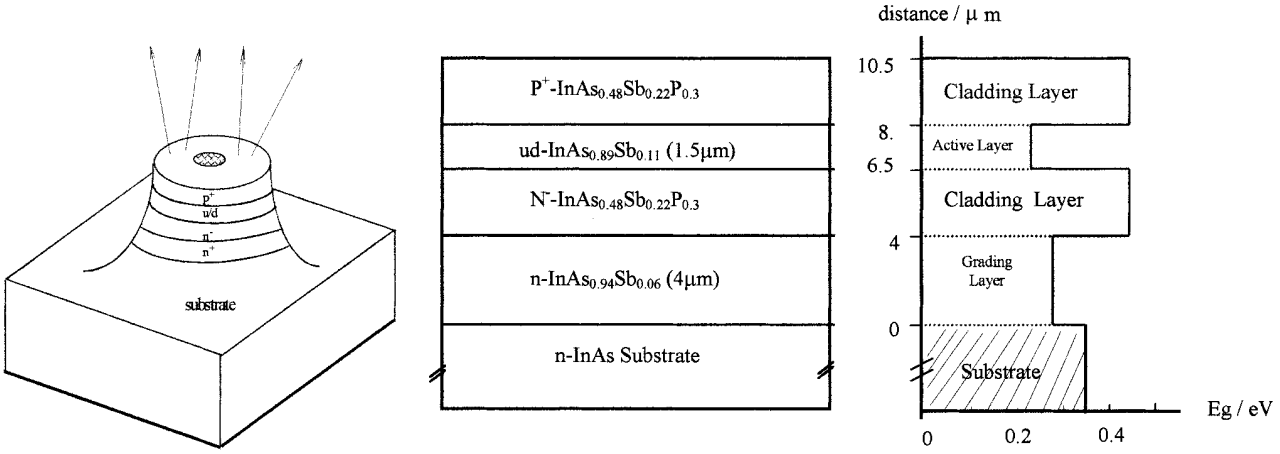

Figure 1. The basic device structure and the energy-band diagram of the InAsSbP/InAsSb double heterostructure LEDs showing the $InAs_{0.94}Sb_{0.06}$ step mismatched buffer layer of intermediate composition.

InAs(100) substrates obtained from Wafer Technology Ltd. The basic structure and associated energy-band diagram of the device is shown in figure 1. The heterostructure consists of two cladding layers of $InAs_{0.48}Sb_{0.22}P_{0.30}$ and an active layer of $InAs_{0.89}Sb_{0.11}$ sandwiched between them. The $InAs_{0.89}Sb_{0.11}$ is positively mismatched by 0.76% with respect to the underlying InAs substrate and if grown directly upon it would lead to a substantial number of threading dislocations and corresponding poor device quantum efficiency. In order to alleviate this an $InAs_{0.94}Sb_{0.06}$ step-grading buffer layer of intermediate composition which has 0.41% positive lattice-mismatch to the substrate was deposited first. The growth melts were prepared by using 7N's pure indium, 6N's pure antimony and undoped polycrystalline InSb, InAs and InP. The buffer layer was heavily doped (n^+-type) with Te up to 1×10^{18} cm^{-3} and was 4 μm in thickness. The quaternary cladding layers were doped to 1×10^{17} cm^{-3} n-type and 1×10^{18} cm^{-3} p-type using Te and Zn, respectively. The active region was grown from an InAsSb melt which was undoped and had previously been baked for 20 h at 750 °C in flowing hydrogen for purification. After this treatment, the residual carrier concentration in the active layer material was measured to be approximately 5×10^{16} cm^{-3} by using Hall effect measurements on clover leaf specimens prepared on p-type InAsSbP for electrical isolation. As shown in figure 1 the thickness of the cladding layers was 2–3 μm and the active region was 1.5 μm in thickness. Each of the melt compositions needed to grow these structures was determined and optimized by the systematic adjustment of Sb, P and As mole fractions. The resulting epitaxial samples were processed into 300 μm diameter surface-emitting LEDs in the normal manner using conventional photolithographic techniques and mesa etching. Ohmic contacts were formed by thermal evaporation of Au on both the p and n sides of the wafer at 180 °C and the LED chips were then mounted onto TO49 headers for testing.

The electroluminescence emission spectra from the LEDs were measured in the range 77 K to 300 K using an Oxford Instruments liquid nitrogen cryostat which enabled fixed temperatures to be selected in this range. Electroluminescence was typically excited in the LEDs using

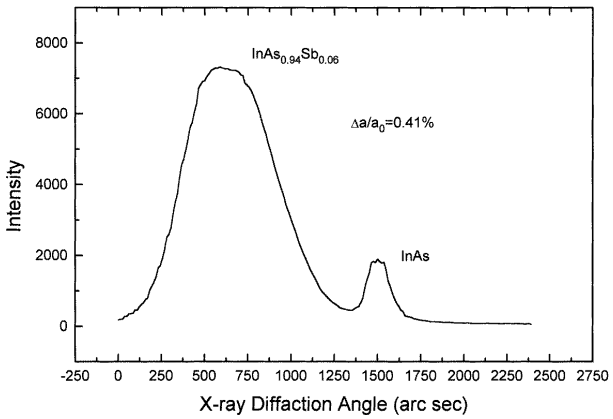

Figure 2. Double crystal x-ray rocking curve for a single $InAs_{0.94}Sb_{0.06}$ epilayer grown on an InAs(100) substrate by LPE, which was used as the buffer layer in our structure.

current pulses of 40 mA at a duty cycle of 20% and a frequency of 250 Hz. After passing through the cryostat windows the radiation was collected using CaF_2 lenses and focused into a 0.3 m Bentham monochrometer. The electroluminescence was detected using a cooled (77 K) InSb photodiode detector and Stanford Research (SR850) digital phase-sensitive detector. A computer was used to control the monochrometer and record the final signal using *Labview* operating software.

3. Results and discussion

Figure 2 shows a double crystal x-ray diffraction curve obtained from a single $InAs_{0.94}Sb_{0.06}$ layer grown on an InAs substrate. The lattice mismatch was measured to be 0.41% and is a very good fit to the structure design. The InAsSb peak is seen to be more intense compared with the InAs substrate simply because it was 5 μm in thickness. The width of the InAsSb peak indicates only a relatively small variation in ternary alloy composition. Optical microscopy revealed that the surface morphology of the whole structure based on the step-grading technique was smooth with only a fine cross-hatch pattern on the surface. An AB-etch of

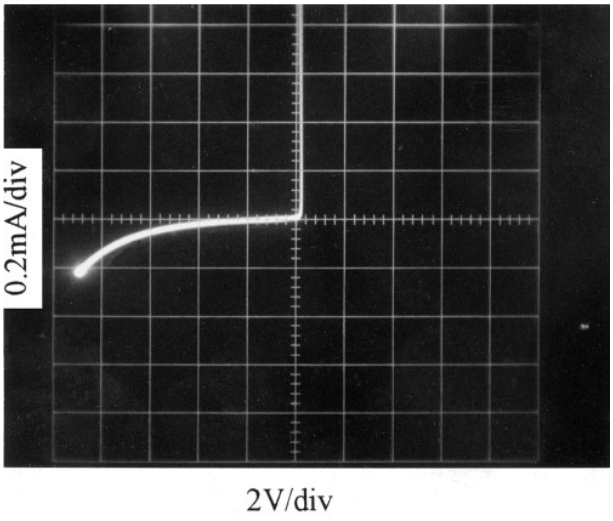

(a)

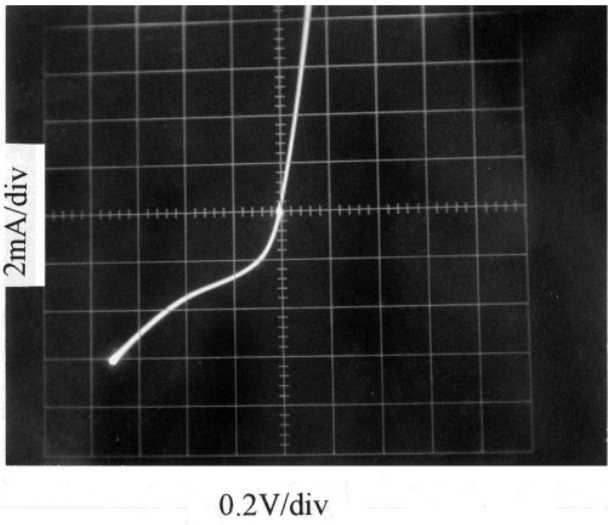

(*b*)

Figure 3. Current–voltage characteristics of one of the InAsSbP/InAsSb LEDs; (*a*) at 77 K and (*b*) at 300 K.

the cross section showed that the interfaces of the complete LED structure were very flat and also that each of the layers was of uniform thickness. Figure 3 shows the I–V characteristics observed from one of the fabricated diodes measured at 77 K and 300 K. The characteristics exhibit the usual exponential rise in forward current, consistent with injection over a potential barrier and the reverse breakdown voltage decreases with increasing temperature as the diode leakage current rises, which is typical for diodes in narrow gap semiconductor materials. As shown in the semi log I–V plot in figure 4, when a low forward voltage (less than 0.02 V) is applied, the ideality factor is near unity, which indicates that diffusion current is the dominant current conduction mechanism. As the applied voltage increases the ideality factor gradually increases to a high value of about 6.5 due to series resistance effects. A plot of the reverse leakage current (at -0.1 V) against inverse temperature is shown in figure 5 for one of the diodes. The equation for the LED reverse leakage current can be written as, $I_R = A\exp(-E_g/kT)$ for diffusion current, changing to

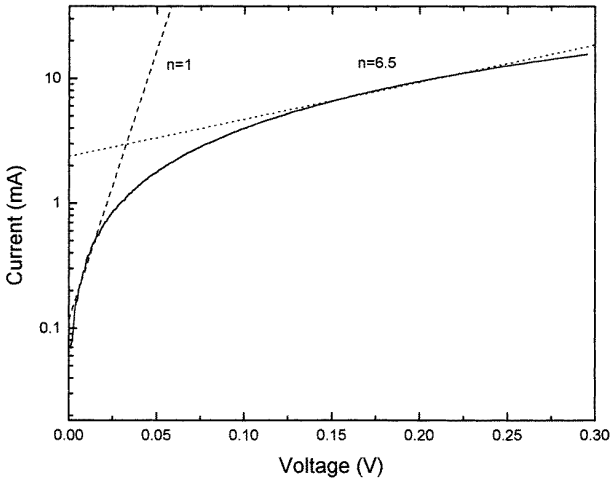

Figure 4. A semi-logarithmic plot of the I–V curve at low forward bias measured at 300 K.

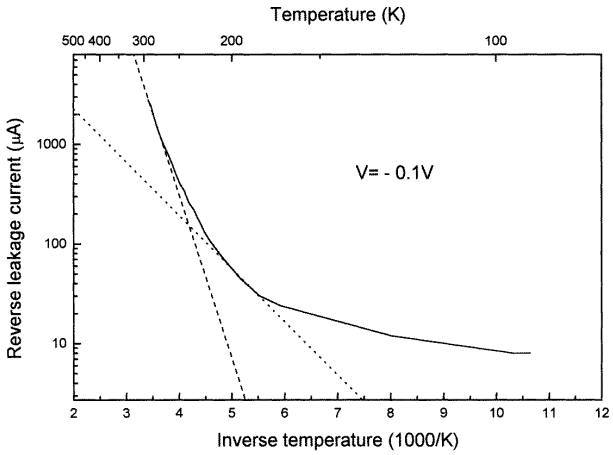

Figure 5. The diode reverse leakage current against an inverse temperature of one of the InAsSbP/ InAsSb LEDs measured at -0.1 V.

$I_R = B\exp(-E_g/2kT)$ when the generation-recombination current dominates, (where A and B are constants and E_g is the bandgap energy of the semiconductor) [20]. The bandgap energy can then be estimated from the slope of $\ln(I_R)$ against inverse temperature. From the slope of the curve near room temperature (and assuming that the diffusion current dominates), we derived a value for the bandgap energy of 0.267 eV, which is in good agreement with that calculated for our $InAs_{0.89}Sb_{0.11}$ ternary alloy at room temperature [21]. At lower temperatures the generation–recombination (G–R) current mechanism takes over as shown in the figure by the second dotted line.

Figure 6 shows the electroluminescence (EL) emission spectra measured from one of our LEDs at different temperatures in the range 80 K to 273 K. As the temperature was increased, the EL emission peaks became broader and moved towards longer wavelengths; but it is noteworthy that no emission from either the quaternary barriers or the buffer layer was observed which indicates that confinement for electrons in the active region is quite good. The absorption near 4.2 μm which is characteristic of CO_2 in the atmosphere ($\sim$0.03%) is clearly evident and is a

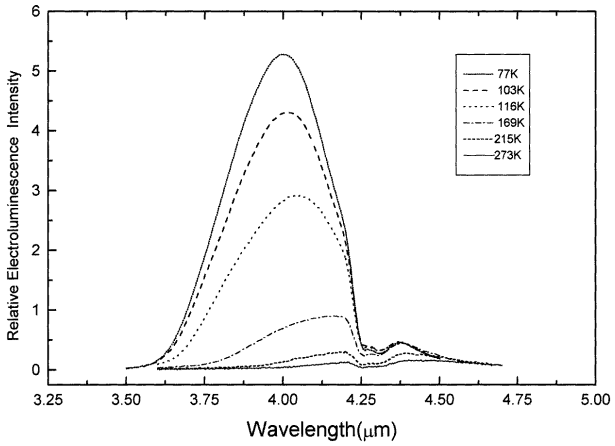

Figure 6. The electroluminescence emission spectra obtained from one of the LEDs measured at different temperatures from 77 K to 273 K. (40 mA peak pulse drive current, 20% duty cycle in each case.)

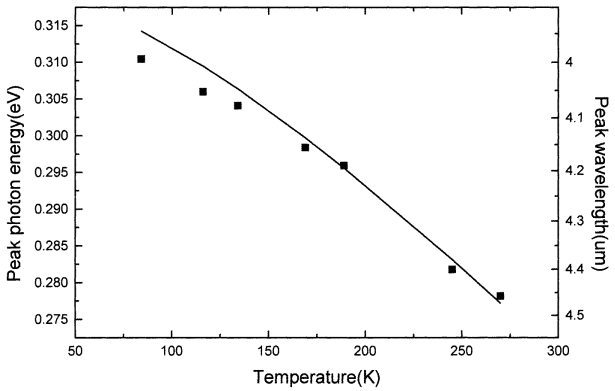

Figure 7. The temperature dependence of the electroluminescence peak emission energy (full squares) of one of the InAsSbP/InAsSb LEDs compared with the theoretical temperature dependence of the band gap (full curve) calculated from [23].

common feature in all the spectra. On increasing the temperature from 77 K to 273 K the peak emission intensity decreased in intensity by approximately a factor of 53. This luminescence quenching behaviour is consistent with increasing competition from non-radiative recombination mechanisms as the temperature increases. In narrow-gap semiconductors such as $InAs_{1-x}Sb_x$ alloys Auger recombination is considered to be the dominant non-radiative mechanism at room temperature [22] while recombination via deep states is more important at 77 K. We also investigated the temperature dependence of the peak emission wavelength from our LEDs. The temperature dependence of the energy gap of the $InAs_{1-x}Sb_x$ alloys has been calculated by Wieder *et al* [23] to be of the form;

$$E_g(x, T) = 0.411\text{–}3.4 \times 10^{-4}T^2/(210 + T) - 0.876x + 0.70x^2 + 3.4 \times 10^{-4}xT(1 - x).$$

Figure 7 shows good agreement between the experimental values (square points) obtained from the EL of our LEDs and the calculated data (full curve) for an x value of 0.115 corresponding closely to the active region composition.

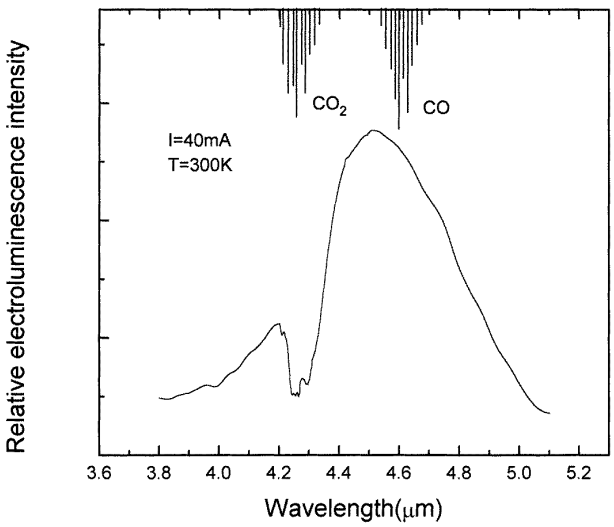

Figure 8. 300 K electroluminescence emission spectrum measured in the laboratory atmosphere from one of the InAsSbP/InAsSb LEDs and the corresponding fundamental CO_2 and CO gas absorptions.

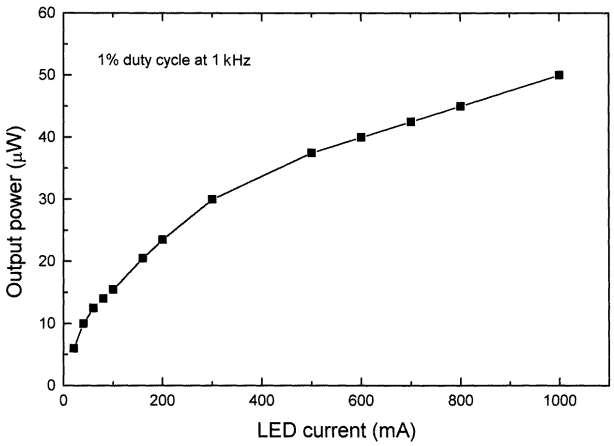

Figure 9. Total power output from one of the InAsSbP/InAsSb LEDs against peak pulse drive current measured using a 1% duty cycle at 1 kHz.

The LED emission at 300 K, with a peak wavelength of 4.5 μm (full width at half maximum = 507 nm) is shown in more detail in figure 8, together with the regions of fundamental absorptions for carbon monoxide and carbon dioxide. The spectrum was measured without flushing the monochromator and clearly shows the strong absorption from CO_2 in the laboratory atmosphere ($\sim$0.03%), whereas CO was not detected. The results indicate that these InAsSb LEDs could form the basis of a portable solid-state CO and CO_2 monitoring instrument. Figure 9 shows the total output power against peak pulse current up to 1000 mA (1% duty cycle at 1 kHz) for a typical 300 μm diameter diode at 300 K. The measurement was performed using a calibrated integrating sphere and 77 K indium antimonide detector. We obtained a room-temperature maximum output power of 50 μW at 1 A and a maximum external power efficiency of 2.7%. The power saturation is indicative of inadequate heat-sinking and imperfect contact resistance which requires further work.

4. Conclusion

We have demonstrated that by using liquid phase epitaxy, it is possible to grow high quality $InAs_{0.89}Sb_{0.11}$ with 0.7% lattice mismatch to InAs by using an intermediate composition buffer layer of $InAs_{0.94}Sb_{0.06}$. Furthermore, this material can be effectively used as the active region within a double heterostructure containing mismatched InAsSbP quaternary barriers to fabricate LEDs. These LEDs operated at 4.5 μm at room temperature and have potential for use in infrared CO and CO_2 gas sensor instruments.

Acknowledgments

The authors would like to thank Kidde International for providing a research studentship for H H Gao and The Royal Society for the visiting fellowship for V Sherstnev.

References

[1] Smith S D, Vass A, Bramley P, Crowder J G and Wang C H 1997 *IEE Proc. Optoelectron.* **144** 266
[2] Tang P J P, Hardaway H, Heber J, Philips C G, Pullin M J, Stradling R A, Yues W T and Hart L 1998 *Appl. Phys. Lett.* **72** 3473
[3] Ashley T, Elliott C T, Gordon N T, Hall R S, Johnson A D and Pryce J G 1994 *Appl. Phys. Lett.* **64** 2433
[4] Stein A, Puttjer D, Behres A and Heime K 1998 *IEE Proc. Optoelectron.* **145** 257
[5] Faist J, Capasso F, Sirtori C, Sivco D L, Hutchinson A L and Cho A Y 1996 *Electron. Lett.* **32** 6
[6] Sirtori C, Faist J, Capasso F, Sivlo D L, Hutchinson A L and Cho A Y 1997 *IEEE Photonics Technol. Lett.* **9** 3
[7] Mao Y and Krier A 1996 *Mater. Optoelectron. Conf. (Sheffield 1995) Optical Mater.* **6** 55–61
[8] Parry M K and Krier A 1994 *Electronics Lett.* **30** 1968–9
[9] Krier A and Mao Y 1997 *IEE Proc. Optoelectron.* **144** 355–9
[10] Popov A A, Sherstnev V V, Yakolev Y P, Baranov A N and Alibert C 1997 *Electron. Lett.* **33** 86–7
[11] Matveev B, Zotova N, Karandashor S, Remenny M, Llinskaya N, Stus N, Shustov V, Talalakin G and Malinen J 1998 *IEE Proc. Optoelectron.* **145** 254
[12] Popov A A, Stepanov M V, Sherstnev V V and Yakovlev Yu P 1998 *Sov. Tech. Phys. Lett.* **24** 596
[13] Esina N P, Zotova A V, Markov I I, Mateev B A, Rogachev A A, Stus N M and Talalakin G N 1985 *J. Appl. Spectrosc.* **42** 465
[14] Skelton J R and Knight J R 1985 *Solid State Electron.* **28** 1166
[15] Mao Y and Krier A 1996 *Electron. Lett.* **32** 479
[16] Grietens B, Nemeth S, Van Hoof C, Van Daele P and Borghs G 1997 *IEE Proc. Optoelectron.* **144** 295
[17] Elies S, Krier A, Cleverley I R and Singer K 1993 *J. Phys. D: Appl. Phys.* **26** 159
[18] Biefeld R M, Allerman A A, Kurtz S R and Burkhart J H 1998 *Institute of Physics Conference Series 156* (Bristol: Institute of Physics) p 113
[19] Biefeld R M, Kurtz S R and Allerman A A 1997 *IEEE J. Selected Topics in Quantum Electron.* **13** 739
[20] Sze S M 1969 *Physics of Semiconductor Devices* (New York: Wiley) section 2.4
[21] Coderre W M and Woolly J C 1970 *Can. J. Phys.* **48** 463
[22] Ciesla C M *et al* 1996 *J. Appl. Phys.* **80** 2994
[23] Wieder H H and Clawson A R 1973 *Thin Solid Films* **15** 217